ADVANCED HEALTHCARE MATERIALS
www.advhealthmat.de

Densification of Type I Collagen Matrices as a Model for Cardiac Fibrosis

*Logan J. Worke, Jeanne E. Barthold, Benjamin Seelbinder, Tyler Novak, Russell P. Main, Sherry L. Harbin, and Corey P. Neu**

Cardiac fibrosis is a disease state characterized by excessive collagenous matrix accumulation within the myocardium that can lead to ventricular dilation and systolic failure. Current treatment options are severely lacking due in part to the poor understanding of the complexity of molecular pathways involved in cardiac fibrosis. To close this gap, in vitro model systems that recapitulate the defining features of the fibrotic cellular environment are in need. Type I collagen, a major cardiac extracellular matrix protein and the defining component of fibrotic depositions, is an attractive choice for a fibrosis model, but demonstrates poor mechanical strength due to solubility limits. However, plastic compression of collagen matrices is shown to significantly increase its mechanical properties. Here, confined compression of oligomeric, type I collagen matrices is utilized to resemble defining hallmarks seen in fibrotic tissue such as increased collagen content, fibril thickness, and bulk compressive modulus. Cardiomyocytes seeded on compressed matrices show a strong beating abrogation as observed in cardiac fibrosis. Gene expression analysis of selected fibrosis markers indicates fibrotic activation and cardiomyocyte maturation with regard to the existing literature. With these results, a promising first step toward a facile heart-on-chip model is presented to study cardiac fibrosis.

1. Introduction

Cardiac fibrosis is a disease state characterized by excessive extracellular matrix accumulation within the myocardium, and is a key element of many cardiac pathologies.[1] One common etiology of cardiac fibrosis is myocardial infarction, where tissue ischemia leads to rapid cell death which triggers an immune response and a subsequent dense, fibrillar scar.[2] Furthermore, hypertrophic cardiomyopathy is also associated with significant cardiac fibrosis, and represents a cardiac fibrosis etiology not preceded by any obvious traumatic event to the tissue.[3] Even less obvious conditions such as diabetes,[4] obesity,[5] and aging[6] have also been shown to introduce progressive cardiac fibrosis. The range of etiology for cardiac fibrosis is indicative of the complex environment of cardiac tissue, suggesting the need for a better understanding of the conditions that can cause cardiac fibrosis symptoms or cellular conditions.

Although commonly associated as a symptom of other pathologies, fibrosis can lead to a number of life-threatening problems. Fibrosis of the myocardium disrupts the excitation–contraction coupling of the heart, causing both diastolic and systolic impairments,[7,8] which can lead to ventricular dilation and systolic failure.[9] Current treatments for cardiac fibrosis are limited and severely lacking. Clinical studies have shown regression of fibrosis and improved diastolic function in hypertension patients treated with angiotensin-converting enzyme inhibitors.[10] Additionally, statin treatment has been shown to significantly decrease fibrosis and hypertrophy in a rabbit model.[11] However, the mechanism responsible for fibrotic regression in these cases remains unknown. The sheer number and complexity of molecular pathways involved in fibrotic activation has severely limited the understanding of the mechanism behind cardiac fibrosis.[12] While several fibrosis animal models exist, they often only resemble partially fibrotic conditions, and are overall costly and time intensive, especially for exhaustive studies. In vitro cellular studies, in turn, are much more suitable for high throughput analysis, drug tests, or gene manipulations. However, to our knowledge, no in vitro model exists that sufficiently recapitulates the complex mechanical and compositional alterations of the extracellular matrix (ECM) environment in fibrotic tissue.

Collagen is the most abundant extracellular protein found within the myocardium.[3] It is responsible for the vast majority of mechanical strength of the matrix while also transmitting the force generated by myocytes. More specifically, type I collagen represents 85% of the collagen content found within the myocardium.[13] In addition, type I collagen is the main component

L. J. Worke, Dr. T. Novak, Dr. R. P. Main, Dr. S. L. Harbin, Dr. C. P. Neu
Weldon School of Biomedical Engineering
Purdue University
West Lafayette, IN, USA 47906
E-mail: cpneu@colorado.edu
J. E. Barthold, B. Seelbinder, Dr. C. P. Neu
Department of Mechanical Engineering
University of Colorado Boulder
Boulder, CO, USA 80309
Dr. R. P. Main, Dr. S. L. Harbin
Department of Basic Medical Sciences
Purdue University
West Lafayette, IN, USA 47906

DOI: 10.1002/adhm.201700114

of fibrotic depositions, making it an attractive matrix candidate for a fibrosis model. However, collagen-based tissue engineered matrices have been historically plagued by poor mechanical strength due to solubility limitations. Plastic compression of collagen substrates has been shown as a means to push past these natural limitations and significantly increase mechanical properties.[14,15] Additionally, recent collagen extraction developments have yielded collagen materials that more closely mimic the cross-linking behavior seen in vivo.[14–16] Such a combination of collagen formulation and plastic compression allows for the development and tunability of matrices that more closely emulate the native state of the tissue.

It has been well established that cardiac output and cardiomyocyte (CM) function are attenuated significantly in fibrotic myocardium. Exploring CM function in vitro remains a challenge, as mature CMs cannot be isolated without destroying the gap junctions necessary for cellular function.[17] Embryo-derived CMs, however, are still adaptable enough to reconnect after digestion and to develop spontaneous beating behavior.[18] Furthermore, embryonic CMs cultured on polyacrylamide gels with varying stiffness have displayed in vivo like beating behaviors on soft gels that mimic healthy tissue (9–14 kPa), but show severely impaired beating behavior on gels with higher stiffness (>35 kPa) comparable to fibrotic tissues.[19] In this study, we explore the potential of compressed collagen matrices as a mechanically and physiochemically relevant model system for cardiac fibrosis by utilizing collagen in conjunction with late stage embryonic CMs.

2. Results

Collagen matrices were prepared as described in the Experimental Section and summarized in **Figure 1**. Compressed matrices showed significantly higher collagen concentrations over the observed depth (100 µm); however, concentrations were highest at the surface and declined linearly with increasing depth (**Figure 2**). Standard curve data remained linear throughout depth ($R^2 > 0.97$ at all depth levels). Confined compression further showed that the bulk compressive modulus was significantly ($p < 0.001$) increased with 39.1 kPa in compressed samples compared to 6.32 kPa in uncompressed samples. Subsequent culturing of embryonic CMs did not significantly change the compressive modulus of either matrix group over a 4 d culturing period during which all data presented in this paper were acquired (Figure S1, Supporting Information).

Microscale studies revealed changes in matrix properties following compression (**Figure 3**). Scanning electron microscopy (SEM) imaging in conjunction with BoneJ analysis revealed that mean fiber thickness and area fraction of collagen fibers in compressed matrices were significantly higher than in the uncompressed ones. However, atomic force microscopy (AFM) measurements of the compressive modulus showed no significant difference between compressed and uncompressed samples. This result was in stark contrast with bulk compressive modulus which increased more than sixfold after compression.

To determine whether compressed collagen substrates could mimic fibrotic cardiac environments, we seeded embryonic CMs on compressed and uncompressed matrices. CMs developed spontaneous beating within 24 h and grew into a confluent, connected sheet within 3 d (Videos S1 and S2, Supporting Information). At that time, CMs were stained with the calcium sensitive dye Fluo4 to determine the influence of compressed collagen matrices on their beating characteristics (**Figure 4**). Cells on uncompressed collagen showed very distinct and synchronized calcium peaks, whereas calcium waves from CMs cultured on compressed substrates appeared flat and asynchronous. Note that inactive cells were already excluded (see the Experimental Section), which was reflected in the lower number

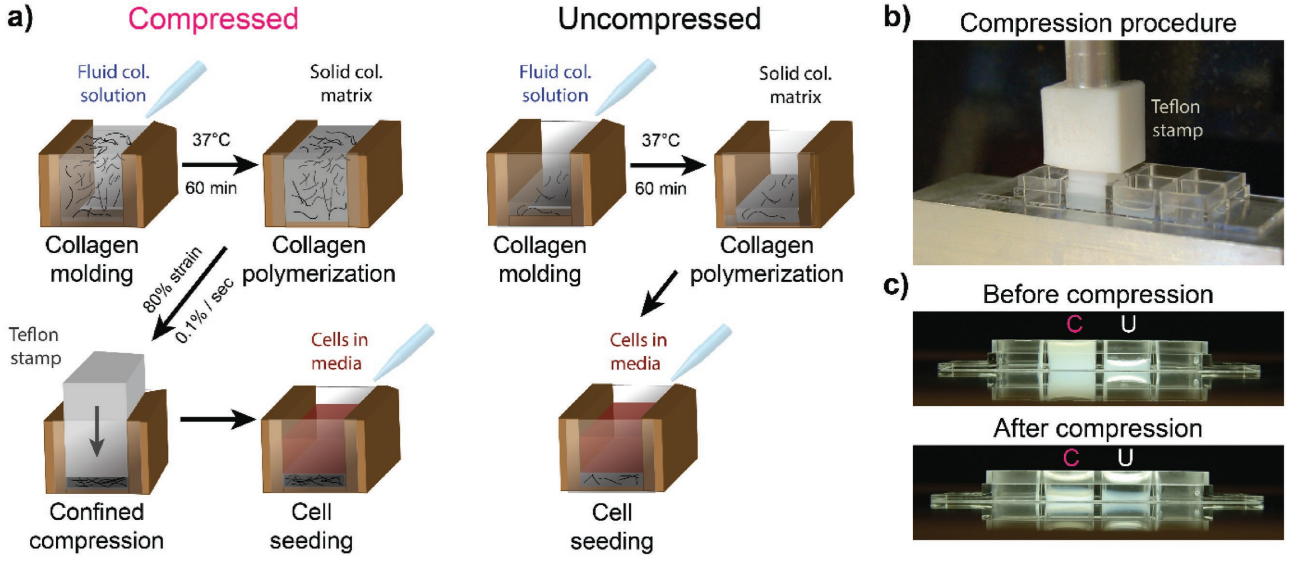

Figure 1. Preparation culturing of collagen matrices. a) Collagen matrices were polymerized with heights of 5 mm (compressed) and 1 mm (uncompressed). Confined compression at 0.1% s^{-1} strain rate resulted in compressed samples of 1 mm final height matching those of uncompressed matrices. Sample wells were then filled with the suspended cell mixture. b) Overview of matrix compression set-up. c) Side view of matrices before (top) and after (bottom) compression, demonstrating equal final height. Please note that the sample on the left undergoes compression.

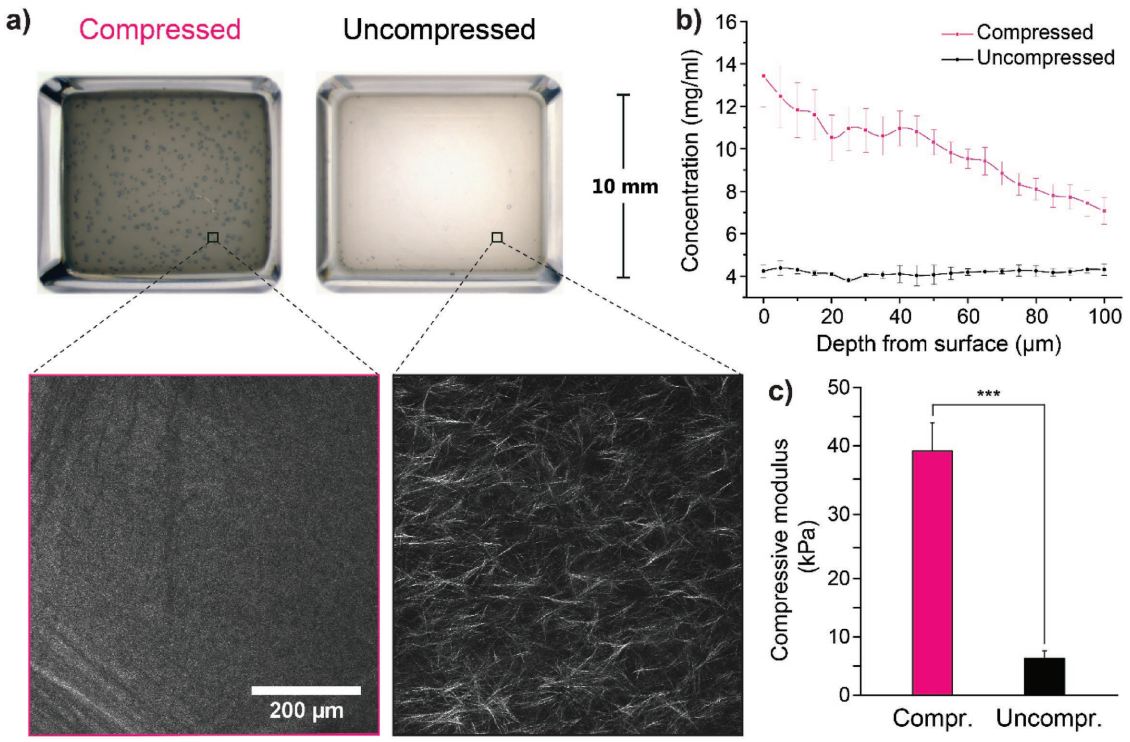

Figure 2. Bulk mechanical properties of collagen matrices. a) A top-down view of matrices postcompression shows increased opacity in compressed samples. Note that the small discolorations in the compressed sample were due to trapped air bubbles. Increased density was similarly seen on the microscale using collagen auto-fluorescence (blow up), where void (dark) regions between individual fibrils in uncompressed samples are lost in compressed samples, as the packing density is increased and the signal intensity becomes more uniform. b) Collagen concentration was significantly increased in compressed samples from the compressive surface to 100 µm into the matrix. Relative density difference between compressed and uncompressed samples decreased with depth. c) Bulk measurement of compressive moduli shows a significant increase in compressed collagen matrices; error bars = SEM, $***p < 0.001$.

of cells observed on compressed matrices. Detailed analysis of calcium signals from cells of four different areas (each) revealed a narrow frequency range of 0.36 ± 0.07 Hz for CMs plated on uncompressed matrices while frequencies on compressed matrices were higher on average but, more importantly, had a wider spread with 0.62 ± 0.20 Hz (Figure 4b). More strikingly, calcium peak intensities (i.e., amplitudes) were on average one magnitude lower for CMs plated on compressed matrices, compared to uncompressed matrices (1.02 ± 0.01 vs 1.23 ± 0.05). Measurement of the individual beat durations during the 20 s time window allowed us to further asses how consistent contractions occur within a single cell, here determined as the coefficient of variation of the time between two contraction peaks. Interbeat variations spanned a wide range from low (3%) to high (130%) for CMs plated on compressed matrices and was on average two times higher compared to uncompressed matrices (51% vs 25%). Surprisingly, despite stark differences in frequency and interbeat variation, average beat durations (full width half maximum) only marginally differed between CMs on both setups (0.88 ± 0.10 s vs 0.78 ± 0.11 s). Calcium wave dynamics, as presented in Figure 4a, further indicated a strong discrepancy in cell-to-cell synchronization for cells plated on compressed matrices. To quantitatively compare this observation, we defined a synchronicity index. First we determined the relative number of cells that beat together at a given time step (Figure 4c, left and middle). This data could then be converted into a single number that represents how synchronized the beats in an area are (1, every cell beats at the same time; ≈0, no cell beats at the same time as another; see the Experimental Section and Equation (1)). As expected, the synchronicity index was distinctly higher for areas recorded on uncompressed substrates compared to compressed ones (0.62 ± 0.14 vs 0.26 ± 0.05).

Next, we wanted to assess if the distinct phenotypic alterations of beating patterns observed on compressed matrices correspond to changes in gene expression using markers that have shown to be relevant in fibrotic pathogenesis by others (**Table 1** and **Figure 5**). In contrast to the observed phenotypic change, widely utilized fibrosis markers showed no change (Actn2), or the opposite of the expected gene expression change (Col1a2, Fgf2, Tgfb1). Interestingly, of the three cardiac-specific fibrosis markers, as determined by a gene profiling study in a fibrosis mouse model,[20] two changed their relative expression as anticipated (Scx, Timp1). Further, two of the four markers that are catalytic mediators of ECM remodeling changed their expression according to previous findings (Timp1, Timp3) while the other two showed the opposite trend (Loxl1, Mmp14). Since we utilized embryonic CMs, and because reactivation of fetal gene programs is an observed phenomena in cardiac fibrosis,[21–23] we additionally monitored the gene response of four established cardiac maturation genes. Expression of Nkx2.5, a cardiac specific transcription factor, and Serca2, a sarcoplasmic

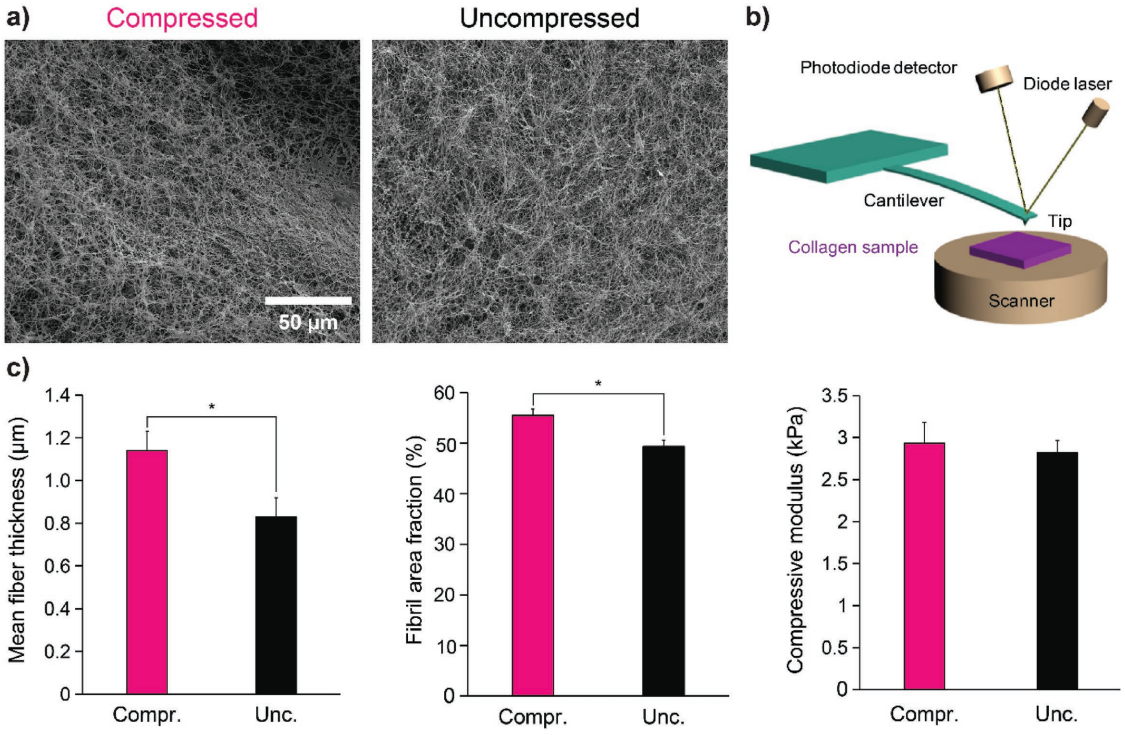

Figure 3. Fibril-level analysis of surface mechanical properties. a) Representative SEM images of compressed and uncompressed matrices. b) Schematic of AFM set-up, where collagen compressive surface was face-up and perpendicular to tip contact. c) Fiber properties as derived from SEM imaging (fiber thickness and area fraction) and AFM measurements (compressive modulus); error bars = SEM, $*p < 0.05$, else nonsignificant.

calcium ATPase that pumps Ca^{2+} ions back into the sarcoplasmic reticulum after contractions, were both increased for CMs cultured on compressed collagen. Similarly, transcription of Myh6, the mature form of the myosin heavy chain found in the contractile sarcomere, was unchanged while the Myh7, the embryonic form, was significantly decreased. Hence all maturation markers indicated a higher progression toward maturation for cells plated on compressed matrices, compared to progression of uncompressed. Finally, since increased inflammation is an issue associated with fibrosis, we tested for the expression change of toll like receptor 4 (Tlr4).[24,25] Against expectations, the inflammation response was downregulated in CMs plated on compressed substrates.

3. Discussion

In this study, we explored the potential of compressed collagen matrices as a mechanically and physiochemically relevant model system for cardiac fibrosis. We found that: (1) changes in the collagen scaffold structure due to compression emulate those seen in the progression of cardiac fibrosis at both the microscale and macroscale, (2) compression of collagen matrices influenced compressive stiffness at the macro scale but not fibril level, and (3) culture of embryonic CM on compressed matrices showed a distinct decline of contractile properties while gene expression analysis of fibrosis-relevant genes was equivocal with respect to fibrotic activation for compressed compared to uncompressed collagen matrices.

Confined compression of collagen matrices showed alterations to the scaffold structure at both the macroscale and microscale in a manner that mimics changes seen in progression of cardiac fibrosis in vivo. Collagen concentration of compressed matrices was significantly increased at the compressive surface. This is consistent with findings of increased type I collagen concentration within fibrotic myocardium.[26] Further, the bulk compressive modulus was significantly increased after compression in accordance with values found in fibrotic tissues. Uncompressed matrices had a compressive modulus similar to healthy (embryonic) heart tissue in vivo (5 kPa here vs 6.32 kPa (embryonic) or 8–60 kPa (adult) in vivo) while compressed matrices were at levels observed for pathologically stiffened tissues (39.1 kPa here vs > 35–144 kPa in vivo).[19,27–30] At the fibril level, compression of collagen matrices showed significant increases in mean fibril thickness and density. Interestingly, this phenomenon is in accord with analysis performed on ECM of fibrotic tissue.[28] Taken together, these results show that compression of collagen substrates is capable of recapitulating a number of defining hallmarks seen in fibrotic tissue.

Compression of collagen matrices had no significant effect on compressive stiffness at the fibril level. Collagen matrices of average fibril thickness on the single micrometer scale were tested with a 10 μm spherical probe, making it likely that only a small number of fibrils were contacting the probe at any given time. At the fibril level, a vast majority of the compressive stiffness is determined by the extent of cross-linking within the matrix.[31] While plastic compression of collagen matrices can increase concentrations past the solubility point, it is a purely

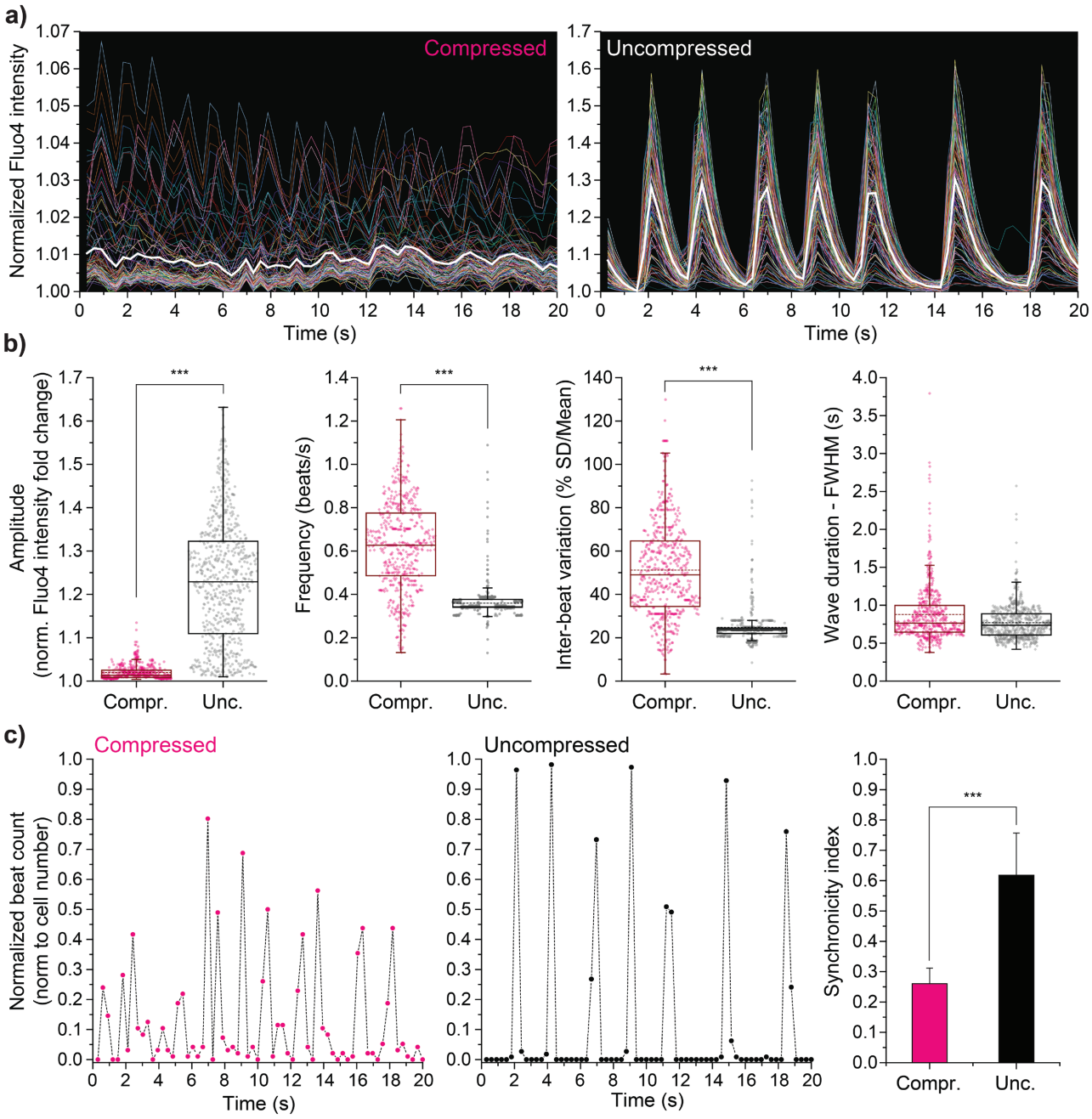

Figure 4. Analysis of calcium staining activity in collagen-plated cardiomyocytes. a) Representative Fluo4-derived calcium signals from one area (≈820 × 820 μm^2) imaged over 20 s at 3.3 fps. Colored lines represent normalized calcium data from each cell (compr. $n = 131$; unc. $n = 147$). Thick white line indicates the average over all cells. b) Cardiac beating properties as calculated from Fluo4-derived calcium wave dynamics using a custom written MATLAB code. For better representation of variation differences, data are shown for all cells (dots) from 4 different areas (compr. $n = 547$; unc. $n = 651$). Statistics, however, was performed on averaged data between areas ($n = 4$). c) Number of contraction peaks for each time step was summed up and normalized over the total cell number (left and middle). From this data, a synchronicity index was generated representing the relative number of cells in an area that beat in conjunction; error bars = SD, ***$p > 0.001$, else nonsignificant.

mechanical effect and therefore lacks the characteristic cross-linking increase seen in cardiac fibrosis.[32] This theory is supported by the increase seen at the bulk scale level, where a significant difference in compressive modulus is observed when the majority of fibers are being engaged and fiber density begins to play a larger role. While increased collagen cross-linking has been shown to be related to matrix stiffening, the complex interplay and relative importance of increased cross-linking versus increased collagen concentration in cardiac fibrosis is yet to be fully understood.[33] Additionally, we were not able to distinguish whether the contractile profile change in CMs was due solely to the compressive modulus, and not

Table 1. List of fibrosis-related gene markers. List of chosen fibrosis-relevant gene markers obtained from literature regarding fibrosis or related heart defect studies in vivo. Primer pair sequences as well as the RefSeq ID used to design primers are shown. Note that references are not the source of the primer sequences as all sequences have been custom designed for this study.

Symbol	Gene name	RefSeq#	Primer pair (5′-3′)	References
Gapdh	Glyceraldehyde-3-phosphate dehydrogenase	NM_008084.3	TGTCAAGCTCATTTCCTGGTATG GGGATAGGGCCTCTCTTGCT	[74,75]
ActB	Actin β	NM_007393.3	GATCAAGATCATTGCTCCTCCTG AGGGTGTAAAACGCAGCTCA	
Acta2	Smooth muscle actin, α-2	NM_007392.3	AGCCATCTTTCATTGGGATGG CCCCTGACAGGACGTTGTTA	[53,57–59]
Col1a2	Collagen I, α-2 chain	NM_007743.2	AGAGGACTTGTTGGTGAGCC TTTCCTTCTTCACCGCTGGG	
Fgf2	Fibroblast growth factor 2	NM_008006.2	GCTGCTGGCTTCTAAGTGTG GTCCAGGTCCCGTTTTGGAT	[37,60]
Tgfb1	Transforming growth factor β-1	NM_011577.2	AGCTGCGCTTGCAGAGATTA AGCCCTGTATTCCGTCTCCT	[47,61]
Scx	Scleraxis, bHLH transcription factor	NM_198885.3	GAGAACACCCAGCCCAAACA TGTCACGGTCTTTGCTCAAC	[20,44–46]
Loxl1	Lysyl oxidase like 1	NM_010729.3	CCTGAGTCCAGGCTGCTATG TTCACGTGCACCTTGAGGAT	[20,62]
Timp1	Tissue inhibitor of metalloproteinase 1	NM_001044384.1	GTGCACAGTGTTTCCCTGTTT GGACCTGATCCGTCCACAAA	[20,40,55]
Timp3	Tissue inhibitor of metalloproteinase 3	NM_011595.2	CAACTCCGACATCGTGATCC CACGTGGGGCATCTTACTGA	[48,49,51,63,64]
Mmp14	Matrix metallopeptidase 14	NM_008608.4	GCCCTCTGTCCCAGATAAGC ACCATCGCTCCTTGAAGACA	[42,48]
Myh6	Myosin, heavy chain 6, cardiac muscle, α	NM_001164171.1	CTCTGGATTGGTCTCCCAGC GTCATTCTGTCACTCAAACTCTGG	[65,66]
Myh7	Myosin, heavy chain 7, cardiac muscle, β	NM_080728.2	CAACCTGTCCAAGTTCCGCA TACTCCTCATTCAGGCCCTTG	
Nkx2.5	NK2 homeobox 5	NM_008700.2	ATTTTACCCGGGAGCCTACG CAGCGCGCACAGCTCTTTT	[67,68]
Serca2	ATPase, sarcoplasmic/endopl. reticulum Ca2+ transporting 2	NM_001110140.3	CCGGCTGAAGAAGGAAAAACC CCACGATTGCATTGGCTACC	[69]
Tlr4	Toll-like receptor 4	NM_021297.3	TGGTTGCAGAAAATGCCAGG AGGAACTACCTCTATGCAGGGAT	[24,25,70]

alternatively or additionally to tensile stiffness, porosity, protein density, or anisotropy, which may be more fully explored in future studies. However, the role of cross-linking versus collagen concentration is further interesting in the light of the decreased Lox1 expression that we found on compressed collagen. Lysyl oxidase like protein 1 catalyzes the formation

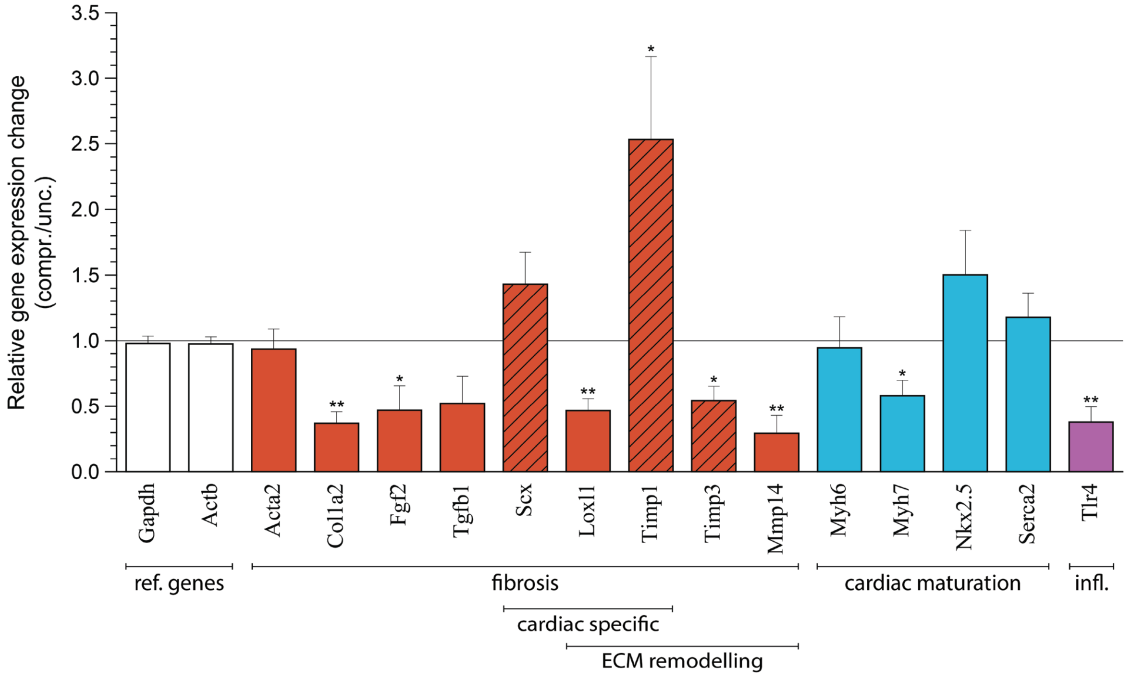

Figure 5. Gene expression analysis of fibrosis marker. After 4 d of culturing, mRNA from CMs plated on compressed or uncompressed collagen matrices were harvested and gene expression of fibrosis-relevant genes was analyzed via qPCR (see also Table 1). All samples were normalized through the established cardiac reference genes Gapdh and Actb. Striped bars indicate genes with gene expression changes similar to the literature. Data are presented as relative expression change for CMs on compressed compared to uncompressed matrices; ref. = reference, infl. = inflammation, $n = 4$, error bars = SEM, $*p < 0.05$, $**p > 0.01$, else nonsignificant.

of crosslinks in collagen and other ECM proteins, and is normally found to be upregulated in fibrosis.[20] The fact that we observed a significant downregulation (2.2-fold) of Loxl1 in our fibrosis model with limited cross-linking capabilities indicates the importance of recapitulating the complex ECM alterations during fibrosis as closely as possible in a fibrosis cell model.

Initial long-term culture studies of CMs on noncompressed matrices showed steady cell activity of CMs well beyond 2 weeks (Video S3, Supporting Information). During this time, after about 7 d of culturing, the edges of the flat sheet matrix started to curve up into a spherical confirmation, thus indicating cell-mediated matrix remodeling. Mechanical testing at 0 and 4 d indeed revealed a slight increase in compressive modulus of both compressed (44.7 ± 8.2 to 48.4 ± 13.1 kPa) and uncompressed (0.9 ± 0.1 to 1.0 ± 0.1 kPa) matrices, however, the changes were not significant ($p > 0.05$) and are expected to have little to no physiological relevance (Figure S1, Supporting Information). Despite the promising stability of the model over the culture times explored in our study, there are still outstanding questions, including: what is the exact time scale over which our approach remains a representative fibrosis model (from a mechanobiology standpoint)? Are other matrix shapes such as spherical or tubular confirmations better suited to provide the physiologically relevant contexts? It may be possible to utilize this system in future studies to model other cardiac conditions over longer time scales in a heart-on-chip like fashion.

Embryonic CMs displayed a strong phenotypic response with beating patterns on compressed matrices showing all the hallmarks of CMs beating in fibrotic tissue: weak calcium amplitudes are indicative of decreased systolic output, high interbeat variation is symptomatic for arrhythmias, and poor cell-to-cell synchronization is reflective of disturbed excitation coupling between cells.[7] Even elevated frequency, observed here as well, is typically a symptom observed in patients with fibrotic heart conditions.[7,34] It remains uncertain, however, if this resembles a physiochemical feedback on the cellular level or a method of the body to compensate for poor systolic outputs in patients. Interestingly, despite distinct alterations in frequency and interbeat variation, beat duration (full width at half maximum, FWHM) remained remarkably unchanged, on average. This is consistent with our results showing unaltered Serca2 (a sarcomeric reticulum calcium ATPase) expression, as its protein manifestation pumps Ca^{2+} ions back into the sarcoplasmic reticulum after contractile excitation and therefore has a prominent influence on contraction durations.

After observing a strong phenotypic change of CMs cultured on compressed matrices, we were surprised to find that most of the fibrosis-related genes we choose to look at showed either no response or the opposite trend expected from literature (Figure 5, nonstriated bars). This is especially true for Acta2, Col1a2, and Tgfb1 as they are frequently utilized as universal fibrosis and stress markers. One reason for this discrepancy could be the use of embryonic CMs in contrast to the adult CMs that are present in the in vivo disease state. This is supported by our findings showing that CMs maturation markers are expressed more highly in CMs plated on compressed collagen matrices which were aimed to resemble fibrotic tissue. The higher mechanical resistance imposed by compressed collagen on the cells might activate parts of a maturation pathway for these CMs similar to the postnatal increase in work load which is known to simulate cardiac maturation.[35] This cascade, in turn, might suppress stress (Tgfb1) and inflammation cascades (Tlr4), as observed here, hence altering the expression of classically observed fibrosis markers. Another reason for the unexpected gene expression, as mentioned above, could be the lack of increased cross-linking or other missing ECM components of our collagen matrices compared to native fibrotic environments. Fgf2 is also normally upregulated in several cardiac conditions due to increased mechanical stress, such as increased hemodynamic load.[36] Studies suggest that Fgf2 is crucial to mount a proper remodeling response when mechanical challenges arise in the heart, further shown by Fgf2 knockout mice suffering from dilated cardiomyopathy.[37] Since Fgf2 expression seems to be positively correlated with mechanical activation, the observed reduction in Fgf2 expression in our study could be attributed to the reduced contractility and therefore reduced mechanical challenge in the compressed collagen matrices.

Despite discrepancies in our gene expression results, genes that have been identified as cardiac specific in PA-1 knockout mice,[20] an established murine model that develops extensive cardiac-specific fibrosis,[38] were amongst the genes that showed expected trends, specifically Timp1 and Scx. While Timp1 has been designated as cardiac specific, studies also show profibrotic features of Timp1 in other tissue such as liver,[39,40] lung,[41] and is a reliable predictor for Dupuytren's disease, a common fibrotic disease that effects finger movements.[42] Its role in cardiac fibrosis, however, might be more significant as it has been linked to overall cardiac remodeling and heart failure.[43] Scleraxis (Scx), in turn, is a transactivator for Col1a2 and other collagen-associated genes. It is highly upregulated in cardiac infarct scars in rats and has shown to be crucial in matrix remodeling and fibrosis.[44–46] The fact that Scleraxis is upregulated while Col1a2 is downregulated in our study is counter intuitive in the light of current literature. Data indicates, however, that Scleraxis works in conjunction with the TGFβ1 pathway, hence the maturation-related abrogation of TGFβ1 as proposed above may also play a role here.[44,47] The third gene that showed gene expression changes in accordance with the current findings was another member of the TIMP family, Timp3. While not designated as cardiac specific, Timp3 has been shown to be consistently downregulated in fibrotic conditions (in contrast to its family member Timp1, which increases). Such studies investigated Timp3 expression in mouse models of age-induced fibrosis,[48] in infarct regions of rat models,[49] and after ischemia in human patients.[50] It was further shown that knock out of Timp3 promotes cardiac remodeling through ECM degradation.[51] This indicates that, even though we did not observe the expected response from all fibrosis marker, the ones that did correspond have shown to play significant roles in fibrosis, leading to the conclusion that part of the fibrotic gene response can be invoked by the presented in vitro fibrosis model.

It is worth mentioning that most fibrosis markers, including Acta2, Col1a2, and most ECM remodeling genes, are expressed by cardiofibroblasts (or their fibrosis-induced transitional equivalents: cardiomyoblasts) in response to soluble factors like TGFβ1 and FGF2 and in response to changing ECM environments.[52] As we deliberately did not purify for CMs (e.g.,

through preplating on TCP) to keep the heterogeneous constitution of cell types as found in the heart, gene expression analysis should be seen as a bulk response from these different cell types. For phenotypic evaluations of this cell culture we choose to focus in this study on CMs as the functionally relevant component. However, it will be important to investigate the cardiofibroblast response too, for example their transition into cardiomyoblasts in fibrotic conditions, as myoblasts are the main driving force for remodeling and a promising target for therapeutics.[53] It is likely that changes in cardiofibroblast behavior had an influence on the observed decline in beating behavior and decreased synchronicity between CMs. Fibroblasts generally tend to proliferate faster on stiffer substrates. Consequently, the lower number of active CMs on compressed matrices detected by the Fluo-4 assay (compr. $n = 547$ vs unc. $n = 651$, see Figure 4) might also reflect an increased number of cardiofibroblasts in the population. Cardiofibroblasts can enhance Ca^{2+} propagation by connecting isolated CMs and even enhance conduction velocities by elevating CM resting membrane potentials. However, the same mechanism causes conduction velocities to decrease and premature simulation of CMs to increase as cardiofibroblasts become more prevalent.[54]

It should further be noted that fibrosis markers not only show divergent results between studies but also have controversial roles or may vary in expression patterns within protein families in a tissue-specific manner. Even a functionally well-defined protein family like MMPs (matrix metalloproteinases), which as proteinases were thought to primarily degrade different ECM structures, have been shown to modulate a range of biological processes other than remodeling. Hence some show profibrotic and others antifibrotic functions.[55] The same is true for their counterparts, the TIMP family (tissue inhibitor of metalloproteinases). Particularly, TIMP3 has been shown to have a significant influence on the balance between cell survival and cell death.[56] Hence the role of single gene expression markers, not to mention the complex interaction between their respective proteins, is far from fully understood. The fact that we observed contradictory responses from established genes, such as decreased expression of Tgfb1 in the light of a strong phenotypic response or downregulation of Col1a2 despite upregulation of its transactivator Scx, highlights the need for a better understanding of the different pathways involved in this complex pathologic phenomena and how they interact with each other. While we aim to improve this system, e.g., through prematuration of embryonic CMs, an in vitro system that mimics only parts of the response is helpful for a differential analysis of many aspects of fibrosis. In our study, the abrogated beating response of CMs, which plays an ultimate role in fibrosis-mediated fatalities, could be studied separately from other aspects of fibrosis.

In conclusion, we have shown that compressed collagen matrices can emulate key features of fibrotic ECM alterations that were able to invoke a strong decline in CM beating performance similar to fibrotic in vivo conditions. While gene expression analysis of CMs was equivocal at first, three genes (Timp1, Timp3, and Scx) that play an important role in fibrosis showed alterations in their expression in accord with fibrosis literature. While more improvements in cell culture and ECM recapitulation need to be made to fully model all in vivo aspects, compressed collagen substrates prove effective to study distinct aspects of cardiac fibrosis, such as the observed abrogation of cardiac contractile properties in this emulated fibrotic environment.

4. Experimental Section

CM Isolation and Culture: CMs were prepared from black 6 (C57BL/6J, Jackson Laboratory) mouse embryos at E18.5 of development. Embryonic hearts were submerged in a 0.125% (w/v) trypsin overnight (12–14 h) at 4 °C with agitation. Digestion solution was removed leaving only residual trypsin, and hearts were digested in 2 mL preheated 37 °C Dulbecco's Modified Eagle's medium (DMEM) F12 (Life Technologies) for 10 min. Digested hearts were pipetted through a 75 µm strainer to remove extracellular material. Cells were plated directly on collagen substrates in DMEM F12 Advanced containing 10% fetal bovine serum and 1% penicillin-streptomycin (Life Technologies) at a density of 500 000 cells cm^{-2}. Samples were incubated at 37 °C and 5% CO_2. Cardiomyocytes formed a spontaneously beating monolayer within 2 d of plating.

Collagen Matrix Preparation: Type I oligomeric collagen from porcine dermis was obtained as previously described.[16] Collagen was solubilized at 4.25 mg mL^{-1} and neutralized with 1.7 M phosphate buffered saline. Glass-bottom 8-well plates (Ibidi) with 1 cm^2 per well surface areas were filled with neutralized collagen to final thicknesses of 1 mm (for uncompressed matrices) or 5 mm (for uncompressed matrices) (Figure 1). Matrices were polymerized at 37 °C for 1 h. Samples in the compressed group were densified within the well using a custom-fit Teflon stamp. Densification was controlled using a Bose ElectroForce 5500 mechanical testing system at a 0.1% s^{-1} strain rate to 80% final strain (1 mm final height). Densification of this magnitude was selected such that mechanical properties of compressed collagen closely matched values reported in the literature for fibrotic tissue (discussed subsequently).

Density Analysis: The density of collagen matrices was characterized via collagen autofluorescence using a 488 nm laser on an Olympus ix81 confocal microscope (Olympus). Collagen matrices of 0, 1, 3, and 4.25 mg mL^{-1} were created for a standard curve ($n = 3$), with 0.1 M HCl serving as the diluent. Matrices were imaged from the surface to 100 µm depth at 5 µm increments, holding all other imaging parameters constant across samples. Settings were chosen such that there was no oversaturation at the highest density regions as well as signal at the lowest density regions. Sum image intensity was recorded at each depth using ImageJ software (NIH) analysis. At each depth level, a linear regression was performed to relate image intensity to collagen concentration. Collagen concentration of compressed samples was determined at each depth using this linear relationship similar to that previously described.[14]

Bulk Measurement of Compressive Moduli: Collagen matrices ($n = 3$, each) were prepared as described above for characterization of bulk mechanical properties. Matrices were tested in confined compression using a Bose ElectroForce benchtop mechanical testing system with a 50 N load cell (Bose). Samples were compressed using a custom-made 1 cm^2 square-faced Teflon indenter. Matrices were initially contacted to a 0.25 N preload, followed by a constant 0.025 mm s^{-1} strain rate to a final 50% percent strain level (0.5 mm total displacement). The linear stress versus strain response was analyzed using linear regression to determine the bulk compressive moduli of matrices.

Atomic Force Microscopy: AFM (Series 5500, Agilent) was utilized to determine the local mechanical properties of collagen matrices. Matrices ($n = 7$, each) were indented perpendicular to the top surface using a triangular silicon nitride AFM cantilever with borosilicate microspheres (spring constant = 0.68 N m^{-1}; sphere diameter = 10 µm; Novascan Technologies). Indentations were performed with at least 10 data points per region and per sample, and an indentation velocity of 15 µm s^{-1}, as previously described.[71] Compressive modulus of

matrices was determined as previously described using a Hertzian contact model.[72]

Scanning Electron Microscopy: Collagen matrices were imaged using SEM to determine the effect of compression on surface fiber density. Collagen matrices (n = 3, each) were submerged in an ethanol bath containing dry ice for 30 min to freeze. Samples were then lyophilized for 24 h. Matrix surfaces were imaged using a Nova NanoSEM (FEI) with an Everhart–Thornley detector at 1300× magnification. For each image, 9 different locations were analyzed for fibril area fraction and mean fibril thickness using BoneJ, a program developed to measure the same properties in trabecular bone and which was similarly used in collagen analysis before.[73]

Fluo4 Calcium Imaging: Intracellular calcium staining was utilized to characterize the beating activity of CMs on compressed and uncompressed collagen matrices. Samples (n = 4, each) were stained 3 d after plating to record the beating activity while avoiding major matrix remodeling. Samples were stained with a 1:60 dilution of Fluo-4 AM cell permeant calcium stain (Life Technologies) for 30 min prior to imaging. Cell calcium activity was recorded at 488 nm using a Nikon Eclipse Ti widefield microscope (Nikon) with a 20× objective lens and an EMCCD camera (Andor). Images were taken over a 20 s time period at 3.3 fps.

Calcium Wave Analysis: Fluorescence images were analyzed using a custom MATLAB code to determine calcium wave dynamics in single cells. Briefly, cell areas were identified and changes in cytosolic calcium were recorded as Fluo4 fluorescence intensity change over time. Curves were then normalized to reflect fold changes (1 = baseline). Amplitude, frequency, interbeat variation, wave duration, and synchronicity index were then calculated for each cell from these calcium dynamics. To distinguish real contraction peaks from small fluctuations seen in catatonic states as frequently observed on compressed matrices, the minimum intensity between two peaks needed to fall at least below 20% of the average peak fold change to be counted as separate events. Cells with less than 3 detected beats in the 20 s time window were excluded and considered inactive. For each cell, calcium wave properties were determined as follows: amplitude as the average fold changes of detected peaks; frequency reflected the mean, inversed time between two peak events; wave duration was determined from the average of FWHM and interbeat variation was defined as the percent standard deviation of the time between peaks over the average time of each cell within the 20 s time window (coefficient of variation in %). To determine the synchronicity index (SI) for one imaged area, first the relative number of cells beating at each time step (B_t) was determined by summing the number of peaks during the current time step and dividing it by the total number of cells observed. If all cells were perfectly synchronized, this value would either be 0 (no cell beats) or 1 (all cells beat) at a given time step. Beat counts were then squared to assign increasing penalties for values further from 1, summed and divided by the average frequency (f_{avg}) of all cells (Equation (1)). The resulting SI value would be 1 given a perfectly synchronized area and would be closer to 0 with decreasing synchronization

$$SI = \sum_{t=0}^{66} B_t^2 / f_{avg} \quad (1)$$

Gene Expression Analysis: Total RNA was extracted from embryonic CMs 4 d after plating using Aurum Total RNA Mini Kit, was reverse transcribed into cDNA via iScript Reverse Transcription Supermix and real-time quantitative PCR was performed with SsoAdvanced Universal SYBR Green Supermix in a CFX96 Touch thermocycler (all kits and devices from Bio-Rad Laboratories) using 10 ng of cDNA as input for each reaction. The cycling protocol was as follows: 98 °C for 30 s, 40 cycles of 98 °C for 10 s, and 60 °C for 20 s followed by a constant increase from 65 to 95 °C in 0.5 °C increments for melting curve analysis. Primers were designed using NCBI primer blast for the indicated nucleotides (Table 1), cross-confirmed in Ensembl gene database using BLASTN and synthesized by IdtDNA. All primers span at least one exon–exon junction to avoid unintended amplification of undigested genomic DNA. Melting curves of each run were analyzed to verify primer specificity. Relative expression change was calculated using the ΔC_t method. All data were normalized to the reference genes Gapdh and ActB as established in previous heart failure studies.[74,75]

Statistical Analysis: All reported measures for calcium imaging, SEM, and substrate deformation were analyzed using a fully nested ANOVA model. Compression level (compressed vs uncompressed) was treated as a fixed effect. The substrate was treated as a random effect. Image number was treated as a random effect nested within substrate because image location was chosen randomly within each individual substrate. Collagen concentration, compressive moduli, and gene expression values were analyzed using a two-sample T-test with groupings of compressed versus uncompressed.

Supporting Information

Supporting Information is available from the Wiley Online Library or from the author.

Conflict of Interest

The authors declare no conflict of interest.

Keywords

density, heart-on-chip, oligomeric collagen, plastic compression, tissue engineering

Received: January 25, 2017
Revised: June 10, 2017
Published online:

[1] B. C. Berk, K. Fujiwara, S. Lehoux, *J. Clin. Invest.* **2007**, *117*, 568.
[2] N. G. Frangogiannis, *Circ. Res.* **2012**, *110*, 159.
[3] K. T. Weber, *J. Am. Coll. Cardiol.* **1989**, *13*, 1637.
[4] J. Asbun, F. J. Villarreal, *J. Am. Coll. Cardiol.* **2006**, *47*, 693.
[5] S. Bharati, M. Lev, *Am. Heart J.* **1995**, *129*, 273.
[6] A. Biernacka, N. G. Frangogiannis, *Aging Dis.* **2011**, *2*, 158.
[7] S. de Jong, T. A. B. van Veen, H. V. M. van Rijen, J. M. T. de Bakker, *J. Cardiovasc. Pharmacol.* **2011**, *57*, 630.
[8] J. S. Janicki, G. L. Brower, *J. Card. Failure* **2002**, *8*, S319.
[9] Y. Iwanaga, T. Aoyama, Y. Kihara, Y. Onozawa, T. Yoneda, S. Sasayama, *J. Am. Coll. Cardiol.* **2002**, *39*, 1384.
[10] C. G. Brilla, R. C. Funck, H. Rupp, *Circulation* **2000**, *102*, 1388.
[11] R. Patel, S. F. Nagueh, N. Tsybouleva, M. Abdellatif, S. Lutucuta, H. A. Kopelen, M. A. Quinones, W. A. Zoghbi, M. L. Entman, R. Roberts, A. J. Marian, *Circulation* **2001**, *104*, 317.
[12] P. Kong, P. Christia, N. G. Frangogiannis, *Cell. Mol. Life Sci.* **2014**, *71*, 549.
[13] B. I. Jugdutt, *Circulation* **2003**, *108*, 1395.
[14] T. Novak, B. Seelbinder, C. M. Twitchell, C. C. van Donkelaar, S. L. Voytik-Harbin, C. P. Neu, *Adv. Funct. Mater.* **2016**, *26*, 2617.
[15] T. Novak, B. Seelbinder, C. M. Twitchell, S. L. Voytik-Harbin, C. P. Neu, *Adv. Funct. Mater.* **2016**, *26*, 5427.
[16] J. L. Bailey, P. J. Critser, C. Whittington, J. L. Kuske, M. C. Yoder, S. L. Voytik-Harbin, *Biopolymers* **2011**, *95*, 77.
[17] E. A. Woodcock, S. J. Matkovich, *Int. J. Biochem. Cell Biol.* **2005**, *37*, 1746.
[18] S. P. Sheehy, F. Pasqualini, A. Grosberg, S. J. Park, Y. Aratyn-Schaus, K. K. Parker, *Stem Cell Rep.* **2014**, *2*, 282.

[19] A. J. Engler, C. Carag-Krieger, C. P. Johnson, M. Raab, H.-Y. Tang, D. W. Speicher, J. W. Sanger, J. M. Sanger, D. E. Discher, *J. Cell Sci.* **2008**, *121*, 3794.
[20] A. K. Ghosh, S. B. Murphy, R. Kishore, D. E. Vaughan, *PLoS One* **2013**, *8*, e63825.
[21] E. J. Cox, S. A. Marsh, *PLoS One* **2014**, *9*, e92903.
[22] M. N. Sack, L. S. Harrington, A. K. Jonassen, O. D. Mjøs, D. M. Yellon, *Cardiovasc. Drugs Ther.* **2000**, *14*, 31.
[23] H. Taegtmeyer, S. Sen, D. Vela, *Ann. N. Y. Acad. Sci.* **2010**, *1188*, 191.
[24] X. Guo, M. Xue, C.-J. Li, W. Yang, S.-S. Wang, Z.-J. Ma, X.-N. Zhang, X.-Y. Wang, R. Zhao, B.-C. Chang, L.-M. Chen, *J. Ethnopharmacol.* **2016**, *193*, 333.
[25] L.-L. Kang, D.-M. Zhang, C.-H. Ma, J.-H. Zhang, K.-K. Jia, J.-H. Liu, R. Wang, L.-D. Kong, *Sci. Rep.* **2016**, *6*, 27460.
[26] J. P. Cleutjens, M. J. Verluyten, J. F. Smiths, M. J. Daemen, *Am. J. Pathol.* **1995**, *147*, 325.
[27] M. F. Berry, A. J. Engler, Y. J. Woo, T. J. Pirolli, L. T. Bish, V. Jayasankar, K. J. Morine, T. J. Gardner, D. E. Discher, H. L. Sweeney, *Am. J. Pathol.* **2006**, *290*, H2196.
[28] J. E. Jalil, C. W. Doering, J. S. Janicki, R. Pick, S. G. Shroff, K. T. Weber, *Circ. Res.* **1989**, *64*, 1041.
[29] R. G. Wells, D. E. Discher, *Sci. Signaling* **2008**, *1*, pe13.
[30] W. Hiesinger, M. J. Brukman, R. C. McCormick, J. R. Fitzpatrick, J. R. Frederick, E. C. Yang, J. R. Muenzer, N. A. Marotta, M. F. Berry, P. Atluri, Y. J. Woo, *J. Thorac. Cardiovasc. Surg.* **2012**, *143*, 962.
[31] L. Yang, K. O. van der Werf, B. F. J. M. Koopman, V. Subramaniam, M. L. Bennick, P. J. Dijkstra, J. Feijen, *J. Biomed. Mater. Res.* **2007**, *82*, 160.
[32] J. W. Holmes, T. K. Borg, J. W. Covell, *Annu. Rev. Biomed. Eng.* **2005**, *7*, 223.
[33] D. Badenhorst, M. Maseko, O. J. Tsotetsi, A. Naidoo, R. Brooksbank, G. R. Norton, A. J. Woodiwiss, *Cardiovasc. Res.* **2003**, *57*, 632.
[34] A. M. Katz, E. L. Rolett, *Eur. Heart J.* **2016**, *37*, 449.
[35] B. H. Eriksen, E. Nestaas, T. Hole, K. Liestøl, A. Støylen, D. Fugelseth, *Early Hum. Dev.* **2014**, *90*, 359.
[36] D. Kaye, D. Pimental, S. Prasad, T. Mäki, H. J. Berger, P. L. McNeil, T. W. Smith, R. A. Kelly, *J. Clin. Invest.* **1996**, *97*, 281.
[37] C. Pellieux, A. Foletti, G. Peduto, J. F. Aubert, J. Nussberger, F. Beermann, H. R. Brunner, T. Pedrazzini, *J. Clin. Invest.* **2001**, *108*, 1843.
[38] A. K. Ghosh, W. S. Bradham, L. A. Gleaves, B. De Taeye, S. B. Murphy, J. W. Covington, D. E. Vaughan, *Circulation* **2010**, *122*, 1200.
[39] Q.-H. Nie, G.-R. Duan, X.-D. Luo, Y.-M. Xie, H. Luo, Y.-X. Zhou, B.-R. Pan, *World J. Gastroenterol.* **2004**, *10*, 86.
[40] H. Wang, F. Lafdil, L. Wang, S. Yin, D. Feng, B. Gao, *Cell Biosci.* **2011**, *1*, 14.
[41] J. Dong, Q. Ma, *Nanotoxicology* **2016**, *1*, 41.
[42] J. M. Wilkinson, R. K. Davidson, T. E. Swingler, E. R. Jones, A. N. Corps, P. Johnston, G. P. Riley, A. J. Chojnowski, I. M. Clark, *Biochim. Biophys. Acta* **2012**, *1822*, 897.
[43] A. Vianello, L. Caponi, F. Galetta, F. Franzoni, M. Taddei, M. Rossi, P. Pietrini, G. Santoro, *CardioRenal Med.* **2015**, *5*, 1.
[44] M. P. Czubryt, *Fibrog. Tissue Repair* **2012**, *5*, 19.
[45] M. Kardasinski, T. Thum, *J. Mol. Cell. Cardiol.* **2009**, *47*, 174.
[46] L. Espira, L. Lamoureux, S. C. Jones, R. D. Gerard, I. M. C. Dixon, M. P. Czubryt, *J. Mol. Cell. Cardiol.* **2009**, *47*, 188.
[47] C. L. Mendias, J. P. Gumucio, M. E. Davis, C. W. Bromley, C. S. Davis, S. V. Brooks, *Muscle Nerve* **2012**, *45*, 55.
[48] M. L. Lindsey, D. K. Goshorn, C. E. Squires, G. P. Escobar, J. W. Hendrick, J. T. Mingoia, S. E. Sweterlitsch, F. G. Spinale, *Cardiovasc. Res.* **2005**, *66*, 410.
[49] E. M. Wilson, S. L. Moainie, J. M. Baskin, A. S. Lowry, A. M. Deschamps, R. Mukherjee, T. S. Guy, M. G. St John-Sutton, J. H. Gorman, L. H. Edmunds, R. C. Gorman, F. G. Spinale, *Circulation* **2003**, *107*, 2857.
[50] Y. Y. Li, A. M. Feldman, Y. Sun, C. F. McTiernan, *Circulation* **1998**, *98*, 1728.
[51] H. Tian, M. Cimini, P. W. M. Fedak, S. Altamentova, S. Fazel, M.-L. Huang, R. D. Weisel, R.-K. Li, *J. Mol. Cell. Cardiol.* **2007**, *43*, 733.
[52] S. van Putten, Y. Shafieyan, B. Hinz, *J. Mol. Cell. Cardiol.* **2016**, *93*, 133.
[53] K. W. Yong, Y. Li, G. Huang, T. J. Lu, W. K. Z. W. Safwani, B. Pingguan-Murphy, F. Xu, *Am. J. Physiol.* **2015**, *309*, H532.
[54] Y. Xie, A. Garfinkel, P. Camelliti, P. Kohl, J. N. Weiss, Z. Qu, *Heart Rhythm* **2009**, *6*, 1641.
[55] M. Giannandrea, W. C. Parks, *Dis. Models & Mech.* **2014**, *7*, 193.
[56] J. D. Lovelock, A. H. Baker, F. Gao, J.-F. Dong, A. L. Bergeron, W. McPheat, N. Sivasubramanian, D. L. Mann, *Am. J. Physiol.* **2005**, *288*, H461.
[57] S. A. Thompson, C. R. Copeland, D. H. Reich, L. Tung, *Circulation* **2011**, *123*, 2083.
[58] D. R. Waisberg, E. R. Parra, J. V. Barbas-Filho, S. Fernezlian, V. L. Capelozzi, *Clinics* **2012**, *67*, 1039.
[59] S. W. M. van den Borne, J. Diez, W. M. Blankesteijn, J. Verjans, L. Hofstra, J. Narula, *Nat. Rev. Cardiol.* **2010**, *7*, 30.
[60] R. D. Guzy, I. Stoilov, T. J. Elton, R. P. Mecham, D. M. Ornitz, *Am. J. Respir. Cell Mol. Biol.* **2015**, *52*, 116.
[61] Y. Purnomo, Y. Piccart, T. Coenen, J. S. Prihadi, P. J. Lijnen, *Cardiovasc. Hematol. Disord.: Drug Targets* **2013**, *13*, 165.
[62] B. López, A. González, D. Lindner, D. Westermann, S. Ravassa, J. Beaumont, I. Gallego, A. Zudaire, C. Brugnolaro, R. Querejeta, M. Larman, C. Tschöpe, J. Díez, *Cardiovasc. Res.* **2013**, *99*, 111.
[63] V. Kandalam, R. Basu, T. Abraham, X. Wang, A. Awad, W. Wang, G. D. Lopaschuk, N. Maeda, G. Y. Oudit, Z. Kassiri, *Am. J. Physiol.* **2010**, *299*, H1012.
[64] M. L. Lindsey, R. Zamilpa, *Cardiovasc. Ther.* **2012**, *30*, 31.
[65] S. Miyata, W. Minobe, M. R. Bristow, L. A. Leinwand, *Circ. Res.* **2000**, *86*, 386.
[66] P. Han, W. Li, C.-H. Lin, J. Yang, C. Shang, S. T. Nurnberg, K. K. Jin, W. Xu, C.-Y. Lin, C.-J. Lin, Y. Xiong, H.-C. Chien, B. Zhou, E. Ashley, D. Bernstein, P.-S. Chen, H.-S. V. Chen, T. Quertermous, C.-P. Chang, *Nature* **2014**, *514*, 102.
[67] I.-M. Chung, G. Rajakumar, *Genes (Basel)*. **2016**, *7*, 2.
[68] E. Dirkx, P. A. da Costa Martins, L. J. De Windt, *Biochim. Biophys. Acta* **2013**, *1832*, 2414.
[69] A. S. Fargnoli, M. G. Katz, C. Yarnall, A. Isidro, M. Petrov, N. Steuerwald, S. Ghosh, K. C. Richardville, R. Hillesheim, R. D. Williams, E. Kohlbrenner, H. H. Stedman, R. J. Hajjar, C. R. Bridges, *Ann. Thorac. Surg.* **2013**, *96*, 586.
[70] N. V. Ermolova, L. Martinez, S. A. Vetrone, M. C. Jordan, K. P. Roos, H. L. Sweeney, M. J. Spencer, *Neuromuscular Disord.* **2014**, *24*, 583.
[71] M. A. McLeod, R. E. Wilusz, F. Guilak, *J. Biomech.* **2013**, *46*, 586.
[72] J. M. Coles, J. J. Blum, G. D. Jay, E. M. Darling, F. Guilak, S. Zauscher, *J. Biomech.* **2008**, *41*, 541.
[73] M. Doube, M. M. Klosowski, I. Arganda-Carreras, F. P. Cordelières, R. P. Dougherty, J. S. Jackson, B. Schmid, J. R. Hutchinson, S. J. Shefelbine, *Bone* **2010**, *47*, 1076.
[74] Q. Li, T. Hu, L. Chen, J. Sun, J. Xie, R. Li, B. Xu, *Mol. Med. Rep.* **2015**, *11*, 393.
[75] A. Martino, M. Cabiati, M. Campan, T. Prescimone, D. Minocci, C. Caselli, A. M. Rossi, D. Giannessi, S. Del Ry, *J. Biotechnol.* **2011**, *153*, 92.

